Attention recruits frontal cortex in human infants

Cameron T. Ellis[a,1], Lena J. Skalaban[a], Tristan S. Yates[a], and Nicholas B. Turk-Browne[a]

[a]Department of Psychology, Yale University, New Haven, CT 06511

Edited by Michael I. Posner, University of Oregon, Eugene, OR, and approved February 17, 2021 (received for review October 14, 2020)

Young infants learn about the world by overtly shifting their attention to perceptually salient events. In adults, attention recruits several brain regions spanning the frontal and parietal lobes. However, it is unclear whether these regions are sufficiently mature in infancy to support attention and, more generally, how infant attention is supported by the brain. We used event-related functional magnetic resonance imaging (fMRI) in 24 sessions from 20 awake behaving infants 3 mo to 12 mo old while they performed a child-friendly attentional cuing task. A target was presented to either the left or right of the infant's fixation, and offline gaze coding was used to measure the latency with which they saccaded to the target. To manipulate attention, a brief cue was presented before the target in three conditions: on the same side as the upcoming target (valid), on the other side (invalid), or on both sides (neutral). All infants were faster to look at the target on valid versus invalid trials, with valid faster than neutral and invalid slower than neutral, indicating that the cues effectively captured attention. We then compared the fMRI activity evoked by these trial types. Regions of adult attention networks activated more strongly for invalid than valid trials, particularly frontal regions. Neither behavioral nor neural effects varied by infant age within the first year, suggesting that these regions may function early in development to support the orienting of attention. Together, this furthers our mechanistic understanding of how the infant brain controls the allocation of attention.

frontoparietal network | attentional cuing | gaze coding | early development | fMRI

Having an attention system that is capable of swiftly orienting to salient events (i.e., stimulus-driven attention) is essential for many behaviors. This is perhaps most true in infancy, during which exploration is thought to be critical (1) and attention allows infants to fully experience learning moments (2). The value of attention in early development might explain why infants are equipped with the capacity to flexibly allocate attention: They can saccade to onsets soon after birth (3), use cues to facilitate orienting (4, 5), and make predictions about upcoming events (6). Yet, how the infant brain supports attention remains a mystery.

An extensive literature in adults could inform our understanding of the neural basis of stimulus-driven attention in infants. Regions collectively referred to as the frontoparietal network, including right temporal parietal junction (TPJ), superior parietal lobe (SPL), lateral occipital cortex (LOC), frontal eye fields (FEF), middle/inferior frontal gyrus (MFG/IFG), and pulvinar, have been implicated in the orienting of stimulus-driven and goal-directed attention (7–10). Other regions including the anterior cingulate cortex (ACC), insula, and basal ganglia, referred to as the cingulo-opercular or salience network (11), have been implicated in the maintenance and updating of task goals. However, the cingulo-opercular network is activated for stimulus-driven attention when the orienting is unexpected (12). Together, this suggests several functionally distinct regions that may be recruited for stimulus-driven attention across the age span.

Yet, the regions that support stimulus-driven attention in adults are anatomically immature in infants (13–16), and functional connectivity between these regions, critical for supporting attention in adults (17, 18), undergoes rapid development in the first year of life (19–24). Indeed, these regions undergo functional changes late into adolescence (17, 18). Furthermore, the regions that support stimulus-driven attention in adults are also recruited for maintaining goals and volitionally directing attention based on them (i.e., goal-directed attention) (25–27). However, goal-directed attention is less developed than stimulus-driven attention in infants (28–31), suggesting immaturity in some parts of infant attention networks. These threads of evidence led to the proposal that some regions, like the MFG/IFG and ACC, are not sufficiently mature in infancy to support attention, and instead, the TPJ, SPL, and FEF are recruited (32). An alternative account suggests that the frontoparietal and cingulo-opercular networks are capable of functioning in early infancy (20, 33, 34), even if there is anatomical immaturity (35).

Existing studies of the infant attention system have been inconclusive about the extent to which the infant brain recruits adult attention networks. Electroencephalography (EEG) with infants suggested that some neural signatures of attention (36, 37) and error processing (33, 38) are adult-like. However, EEG has insufficient spatial resolution to resolve which regions are supporting attention. Functional near-infrared spectroscopy (fNIRS) offers potentially greater resolution (6, 39), but is unable to localize activity beyond regions close to the scalp surface, including deeper, ventral, medial, and subcortical structures such as the ACC and basal ganglia. Moreover, many aspects of attention behavior develop throughout infancy (40), such as disengagement (41), inhibition (42), and goal-directed attention (28–31), raising the expectation that the underlying brain systems would

Significance

Infants are capable of deftly allocating attention to new information. However, the brain regions that support attention in adults are thought to be immature early in life. We tested awake behaving infants in their first year using gaze coding and fMRI to collect simultaneous behavioral and neural measures of attentional cuing. We found a robust validity effect in behavior from all infants, accompanied by engagement of portions of the brain networks that support attention in adults, notably, regions of frontal cortex. This evidence of maturity is compatible with the importance of attention in scaffolding learning and understanding. This study also highlights the opportunities and challenges of awake infant fMRI, including limitations in experimental design, data collection, and data analysis.

Author contributions: C.T.E. and N.B.T.-B. designed research; C.T.E., L.J.S., T.S.Y., and N.B.T.-B. performed research; C.T.E. and T.S.Y. analyzed data; C.T.E. and N.B.T-B. initially created the protocol; C.T.E., L.J.S., T.S.Y., and N.B.T.-B. collected the data; and C.T.E., L.J.S., T.S.Y., and N.B.T.-B. wrote the paper.

The authors declare no competing interest.

This article is a PNAS Direct Submission.

[1]To whom correspondence may be addressed. Email: cameron.ellis@yale.edu.

This article contains supporting information online at https://www.pnas.org/lookup/suppl/doi:10.1073/pnas.2021474118/-/DCSupplemental.

Published March 16, 2021.

also show age-dependent changes. Hence, it remains unclear how stimulus-driven attention is supported in the infant brain.

We used functional magnetic resonance imaging (fMRI) and offline gaze coding to investigate the behavioral and neural basis of stimulus-driven attention in awake behaving infants under a year old. Among noninvasive techniques, fMRI is uniquely capable of resolving brain-wide, fine-grained attention processes. Recent innovations have made it possible to collect data from awake behaving infants (43–46). Using a developmental variant (4, 47) of the Posner cuing task (48), we simultaneously recorded gaze behavior and whole-brain fMRI activity to uncover the neural basis of attention in infants.

Results

We administered a cuing task while simultaneously collecting fast event-related fMRI to examine how the brain supports stimulus-driven attention in 24 sessions from 20 awake behaving infants aged 3 mo to 12 mo old (*SI Appendix*, Table S1). On each trial, participants saw a brief cue followed by a salient, spinning pinwheel target (4). To assess behavioral evidence of attention, we measured the response time (RT) of saccades to the target (Fig. 1*A*). This target appeared on the left or right side of the display equally often. On 50% of trials, the target was preceded by a cue that appeared on the same side as the target (valid trials). On 25% of trials, the cue appeared on the opposite side from the target (invalid trials), and on the remaining 25% of trials, the cue appeared on both sides (neutral trials). This balancing of trial types meant that the target location was uniquely identified by a cue half of the time (valid trials) and was not for the other half (neutral and invalid trials).

We quantified RT to the target for each of these trial types separately. Our main behavioral index of stimulus-driven attention was the RT difference between invalid and valid trials (Fig. 1*B*). All participants looked to the target faster, on average, on valid than invalid trials (invalid > valid in 24/24 sessions, mean [M] = 0.19 s, 95% CI = [0.16, 0.22], $P < 0.001$). This difference could be driven by a benefit of valid cues facilitating RT, a cost of invalid cues slowing RT, or the combination of both. We found evidence for facilitation by comparing valid with neutral trials (neutral > valid in 23/24 sessions, $M = 0.13$ s, CI = [0.10, 0.16], $P < 0.001$). We also found evidence for slowing by comparing invalid with neutral trials (invalid > neutral in 21/24 sessions, $M = 0.06$ s, CI = [0.03, 0.09], $P < 0.001$).

We interpret the differences in RT between conditions as showing that infants' attention was exogenously captured by the salient cues. However, because valid cues were more frequent than invalid cues, an alternative possibility is that the infants learned to expect a target would appear in the same location as the cue. If true, effects may be diminished in the first block before sufficient exposure had accrued to learn this contingency. We therefore analyzed this first block in isolation (*SI Appendix*, Fig. S1). The results were similar to all blocks, inconsistent with an interpretation of the cuing effects based on learned expectations.

An important consideration is the speed of the saccades, especially on valid trials. It typically takes 300 ms to 500 ms for an infant to initiate and complete a saccade (3, 4), yet a large proportion of trials had RTs much faster than that (*SI Appendix*, Fig. S2*A*) (47). This suggests that infants initiated a saccade immediately after the cue appeared, rather than waiting for the target to appear. Nevertheless, what is important is that these cues were robust drivers of stimulus-driven attention, showing that infants are spontaneously using the cues to allocate attention.

The attention effects observed in the full sample did not vary by age (Fig. 1*C*). Namely, the RT differences between trial types were not reliably correlated with age in months (invalid > valid: $r = 0.17$, $P = 0.352$; neutral > valid: $r = 0.23$, $P = 0.314$; invalid > neutral: $r = -0.03$, $P = 0.873$). That said, older participants were faster overall (*SI Appendix*, Fig. S2*B*; $r = -0.63$, $P < 0.001$), demonstrating that we had sensitivity, in principle, to detect large age effects. We are cautious about drawing a definitive conclusion from null effects, and a larger sample size may reveal a more subtle relationship. However, these findings are consistent with the possibility that cuing effects are stable between 3 and 12 mo of age.

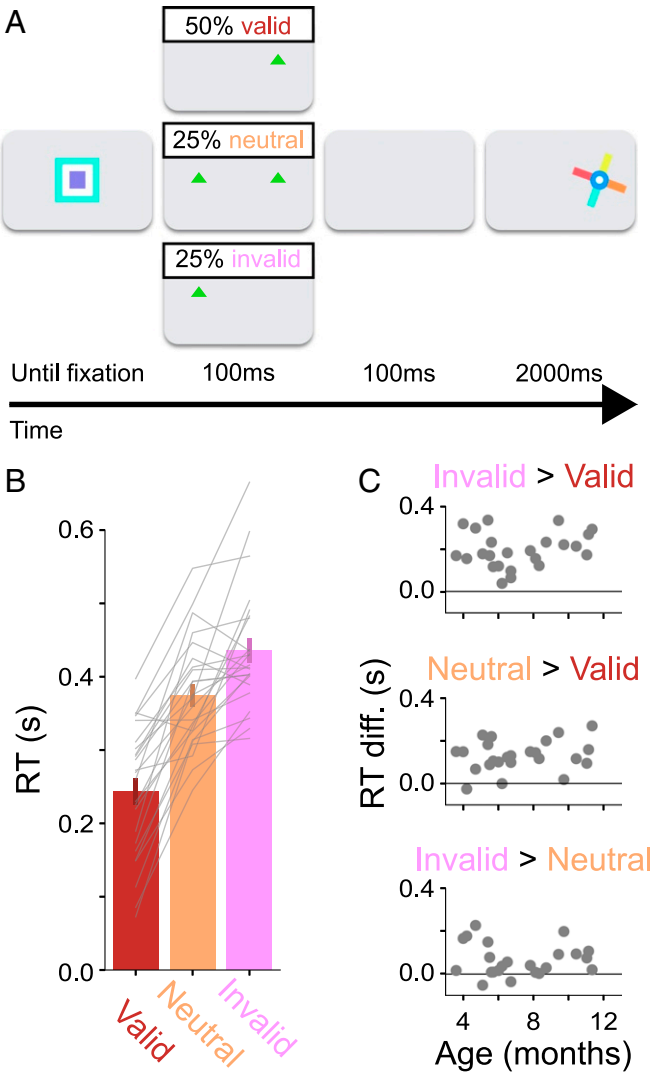

Fig. 1. Task design and behavioral evidence of stimulus-driven attention in infants. (*A*) Trial sequence: Participants were presented with an attention getter until they fixated. A cue was then presented briefly before a target appeared. The cue was either in the same location as the target (valid), in the opposite location (invalid), or cues were presented bilaterally (neutral). (*B*) Average RT in seconds for each trial type. Error bars indicate SE across sessions. Gray lines connect individual session data across the three trial types. (*C*) Relationship of different condition comparisons to age in months.

We investigated the neural mechanisms supporting stimulus-driven attention in infancy using a univariate general linear model (GLM) that contrasted evoked responses for the valid, neutral, and invalid trials (8). The contrast of invalid > valid captured both the costs and benefits of orienting attention to the cue. The costs are isolated by the contrast of invalid > neutral, which would reflect the need to reorient attention given the mismatch between the cue and target locations. The benefits are isolated by the contrast of neutral > valid, which would reflect facilitation of attention by the preparation afforded by the cue appearing at the location of the future target.

Our primary analyses involved planned comparisons within regions of interest (ROIs) from adult attention networks. However, because awake infant fMRI is new and challenging, as a first pass, we conducted an exploratory voxelwise whole-brain analysis to verify that we were able to collect data of reasonable quality and that the cuing task drove responses in the infant brain. This analysis also provided a helpful visualization of the data that was not dependent upon the ROIs, given the problem of aligning adult ROIs in the infant brain. For each comparison between trial types, we calculated the t statistic across sessions in each voxel (Fig. 2). Widespread activity that distinguished between trial types was observed at a liberal threshold not corrected for multiple comparisons. We quantified this activity with greater precision and sensitivity by averaging across voxels within key ROIs.

To test whether regions from adult attention networks were recruited in infants, we defined seven ROIs (*SI Appendix*, Table S2) independently, based on a functional atlas (49), and compared each contrast across sessions (Fig. 3). We used regions that are broadly implicated in attentional processes in adults, beyond just stimulus-driven attention, because the regions that support attention in infants may be different in function than adults, including as a result of the prolonged development of goal-directed attention (50). The planned contrast of valid and invalid trials, which tests the combined benefit of an accurate cue (valid trials) and the cost of an inaccurate cue (invalid trials), resulted in significantly higher activity for invalid trials in LOC (M = 0.47, CI = [0.05, 0.87], P = 0.032), right ACC (M = 0.37, CI = [0.04, 0.70], P = 0.027), and right MFG (M = 0.40, CI = [0.05, 0.76], P = 0.028), and marginally higher activity in right TPJ (M = 0.40, CI = [−0.03, 0.79], P = 0.066). These ROI analyses were planned comparisons and were not corrected for multiple comparisons. That said, finding a significant result in three independent ROIs was unlikely to occur by chance (see *SI Appendix*, *Supplementary Text*). The contrast of valid and neutral trials, which isolates the benefit of facilitation by the cue, yielded significantly higher activity for neutral trials in right ACC (M = 0.37, CI = [0.03, 0.69], P = 0.033) and LOC (M = 0.47, CI = [0.09, 0.84], P = 0.017), and marginally higher activity in intraparietal sulcus (IPS) (M = 0.38, CI = [0.00, 0.72], P = 0.051). The contrast of invalid and neutral trials, which isolates the cost of reorienting when the target appears away from the cue, resulted in no significant regions. The results of these contrasts against neutral trials suggest that overall neural differences between invalid and valid trials, which could have, in principle, measured costs and/or benefits, reflected facilitation from orienting attention to the cue prior to the target. We also did not find that these results correlated significantly with a measure of the amount of data per participant (number of invalid trials; *SI Appendix*, Fig. S3). In sum, regions thought to

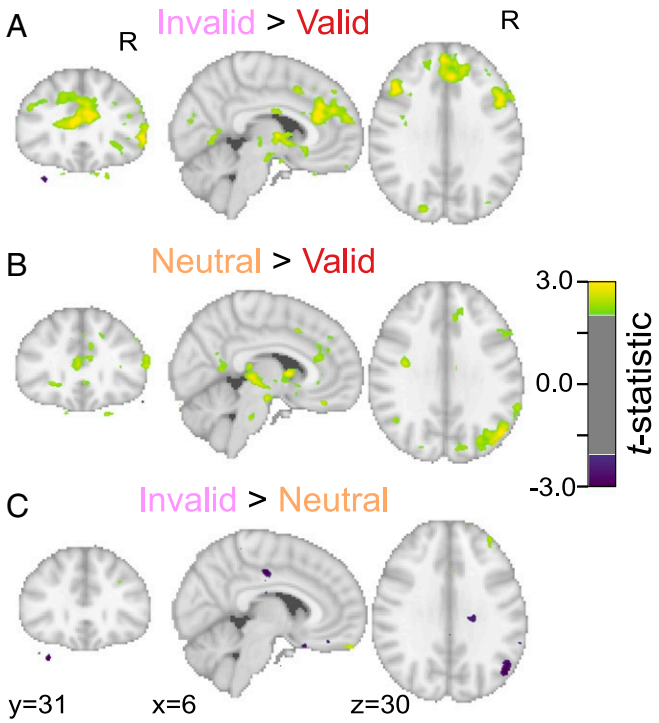

Fig. 2. Whole-brain statistical map of difference between conditions. Contrasts for each session were aligned to standard space and tested for reliability with a group t test. Three tests were performed: (*A*) invalid > valid, (*B*) neutral > valid, and (*C*) invalid > neutral. An uncorrected threshold is used for visualization (P < 0.05). Coordinates are in adult MNI space.

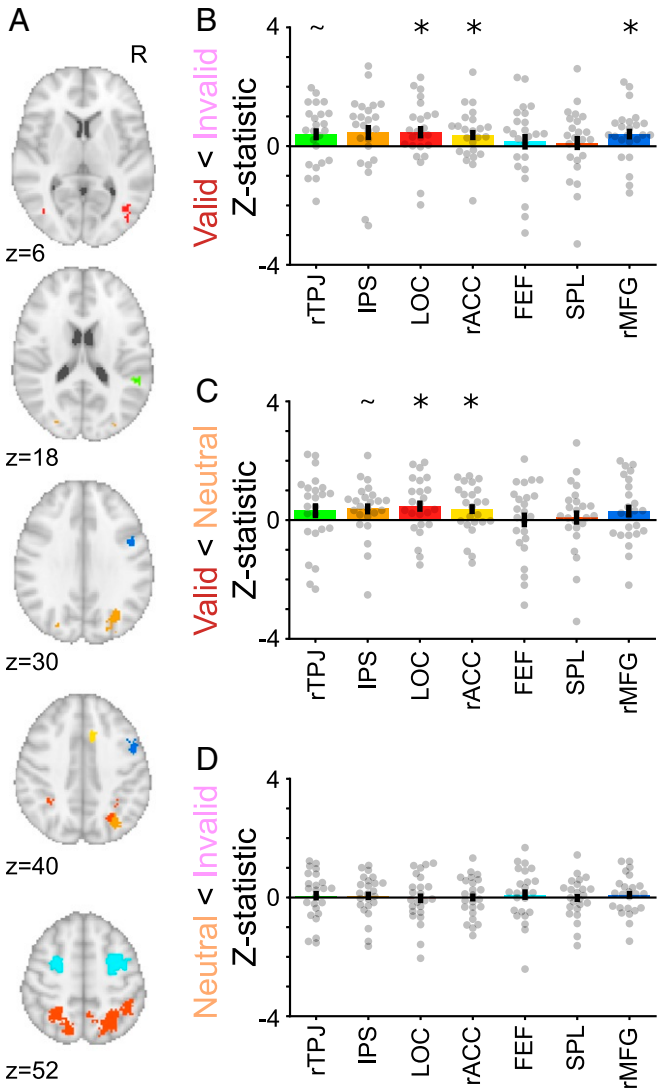

Fig. 3. Neural evidence of stimulus-driven attention in infants. (*A*) Individual ROIs from functional analysis with coordinates in MNI space. Contrasts were extracted from these ROIs, averaged across voxels, and tested for reliability with bootstrap resampling. Three tests were performed: (*B*) invalid > valid, (*C*) neutral > valid, and (*D*) invalid > neutral. Lowercase "r" and "l" indicate left and right hemispheres, respectively. Error bars indicate SE across sessions. * = P < 0.05, ~ = P < 0.075.

support attention in infancy, such as SPL and FEF (32), were not recruited for stimulus-driven attention, whereas regions thought to be immature did support stimulus-driven attention.

Some of these ROIs were small, which could lead to unstable estimates of the average evoked response in different conditions and explain why only a subset of the regions reached significance in different contrasts. However, dilating the ROIs to increase their size yielded very similar results (*SI Appendix*, Fig. S4). Moreover, if we use a spherical ROI around the peak of each functional ROI, thus balancing the number of voxels averaged per region within hemisphere, the results were also similar (*SI Appendix*, Fig. S5). These analyses used linear alignment to standard space, but we found qualitatively similar results substituting nonlinear alignment in the step of registering each infant's anatomical data to the age-appropriate infant template (*SI Appendix*, Fig. S6). Together, these findings suggest that frontal, occipital, and, to a lesser extent, parietal regions are recruited to support stimulus-driven attention in infants.

To provide further evidence for the involvement of these regions in attention, we tested their relationship with the magnitude of behavioral effects. Namely, we correlated the contrast of invalid > valid brain activity with the difference in invalid > valid RT for the three ROIs that showed a significant overall effect. We found reliably negative brain–behavior correlations in right ACC and right MFG, with greater neural differences associated with smaller behavioral differences (*SI Appendix*, Fig. S7). Thus, these regions have functional relevance for behavior, and the direction of the effect may suggest a compensatory relationship, with greater recruitment when attention is weak (18). At the same time, we did not observe any evidence that the strength of the invalid > valid neural contrast correlated with participant age (*SI Appendix*, Fig. S8). This suggests that there may not be developmental changes in stimulus-driven attention across our age range. If we had tested younger infants, covered the whole lifespan, or tested a different aspect of attention (e.g., goal-directed), changes might have been seen (40).

The analyses above used ROIs defined from metaanalyses of adult fMRI studies. This approach assumes that there is a consistent anatomical mapping from adults to infants in Montreal Neuroscience Institute (MNI) standard space. However, we did not expect that alignment would fully recover the large anatomical (and functional) differences between adults and infants. To avoid such assumptions, we performed an additional analysis using cross-validation within the infants to define ROIs in an unbiased, data-driven way. Specifically, we performed a leave-one-out analysis in which clusters of voxels were defined in all but one session, and then the evoked responses from those clusters were quantified in the remaining participant (*SI Appendix*, Fig. S9) (51). Even though we did not make assumptions about where we would find differences, these analyses implicated similar regions in the frontal lobe, including the ACC and IFG. Consistent with the whole-brain analysis (Fig. 2), we found involvement of the basal ganglia, especially the caudate and thalamus, which is part of the cingulo-opercular attention network (11).

In this task, infants allocated attention with eye movements, so it is possible that the differences between conditions were driven by eye movements rather than attention per se (52). In particular, more saccades were made on invalid trials ($M = 2.10$) compared with valid ($M = 1.75$, difference CI = [0.20, 0.50], $P < 0.001$) and neutral trials ($M = 1.84$, difference CI = [0.10, 0.42], $P = 0.001$). To evaluate this possibility, we tested whether saccades themselves evoked responses in the ROIs defined previously (Fig. 3*A*). We ran a separate GLM with a saccade regressor in which events were defined every time the participant moved their eyes. None of the attention ROIs were significantly activated by saccades (*SI Appendix*, Fig. S10*B*). As a positive control to validate this analysis, nonattention regions in early visual cortex were activated (*SI Appendix*, Fig. S10*A*) (53).

Discussion

We investigated the neural mechanisms of stimulus-driven attention in infants under the age of 12 mo. We found robust behavioral evidence that infants allocated attention to cues in our task. We tested whether this attention behavior was supported by regions of frontoparietal and cingulo-opercular networks that are involved in analogous tasks in adults. Posing a challenge to existing theories (32), infant attention recruited regions of the cingulo-opercular network, such as the ACC and basal ganglia, as well as anterior portions of the frontoparietal network, including the MFG/IFG. We used multiple independent analyses to support these conclusions. The results were selective to specific task contrasts and regions, related to behavioral performance, and not reproduced by saccades alone. This supports a growing consensus (33–35, 54) that the human brain may have a surprisingly functional frontal cortex in the first year of life.

The engagement of regions from well-characterized attention networks may help interpret our findings, based on the functions of these regions in adults. The MFG/IFG has previously been implicated in reorienting attention (7, 8, 12, 25, 26) and is considered a highly connected node for distributing information in the frontoparietal network (55). The involvement of the ACC is more surprising, given its role in cognitive control (56) and goal maintenance (11) in adults. These functions have protracted developmental trajectories into late adolescence (57). The ACC (along with the basal ganglia) is not typically recruited for variants of the Posner cuing task (ref. 12, although see ref. 58). Even so, the ACC is part of the salience network (59), which has reliable functional connectivity early in infancy (19, 23, 24). This raises the interesting possibility that the function of the ACC may be different in infants compared with adults. Indeed, children show greater activity than adults in a cluster near the ACC for reorienting of attention (18). An alternative explanation for the involvement of the ACC might be that it detects invalid trials as a violation of expectation. There is some evidence that infants recruit frontal cortex for such error processing (33, 38). Furthermore, the ACC has previously been implicated in orienting attention in adults but only when the orienting is surprising (12, 58), as would happen on invalid trials. Further work is needed to adjudicate the precise function of the ACC in infancy. Nevertheless, our results suggest that frontal regions are involved in allocating attention in infancy despite their protracted anatomical development (13–16).

Although we found recruitment of frontal regions in stimulus-driven attention, we observed noticeably weaker evidence in parietal regions, including the right TPJ. The TPJ allows the adult attention system to disengage from its current focus (7), as would be needed to support reorientation in this task. One reason the TPJ may not have been involved more robustly is that TPJ is particularly important for goal-directed attention (25, 26, 60–63), rather than stimulus-driven attention as tested here. However, infants have diminished goal-directed attention relative to adults (28–31), and the TPJ is recruited more strongly in adulthood than childhood (18). From this perspective, our results might offer circumstantial evidence of the link between TPJ and goal-directed attention (50). An alternative possibility is that the TPJ ROI was small and so may have been more affected by misalignment between participants. However, our supplemental analyses with dilated and spherical ROIs and enhanced nonlinear alignment undermine this possibility. Future studies could compare goal-directed and stimulus-driven attention using fMRI within the same infant participants to determine how these different modes of attention interact and develop.

In this research, there are important limitations to consider. One concern is that the valid trials were more frequent than each of the neutral and invalid trials, potentially allowing infants to learn that the location of the cue predicted the location of the target. If so, shifts in attention may not be caused only by the salience of the cue (i.e., stimulus-driven) but also by this expectation. However, we found behavioral evidence of attention even in the first block of trials, when it was unlikely that sufficient experience had accrued to learn this expectation. Nevertheless, it remains possible that expectation contributed to the behavioral or neural effects. This might still be considered evidence of orienting attention, albeit not exclusively in a stimulus-driven manner. A different consequence of this condition imbalance is that the behavioral and neural contrast between neutral and invalid trials is based on fewer trials than contrasts involving the more numerous valid trials, and thus may have been relatively underpowered.

Another limitation to consider is that our sample size was small for evaluating individual differences based on age or behavior (64). Although sufficiently powered to find significant correlations in our data, such as between neural and behavioral effects and between overall RT and age, small or moderate age effects would require a larger sample size in future studies. For instance, in a large sample, the RT difference of neutral > valid showed a small but significant increase from 5 mo to 7 mo of age (47). That said, many of the components of stimulus-driven attention are thought to be mature by 4 mo of age, whereas other aspects of attention are expected to develop over infancy (40). A related concern is that we excluded 31% of the participants we sampled because they had insufficient usable data. This may have introduced a selection bias, resulting in a final sample with more advanced attention abilities capable of sustaining attention in the task. The behavior of these excluded participants revealed evidence of attentional orienting, albeit weaker than in the included participants (see *SI Appendix*, *Supplementary Text*). Also included in our sample were second sessions from four participants who were scanned weeks to months after their first session. We treated these second sessions as distinct, but this mixing of a little longitudinal data with primarily cross-sectional data could have unintended statistical consequences, such as obscuring the age effects we tested. However, when we used only the first session of data from each participant, so that each session was a unique individual, age effects did not emerge (see *SI Appendix*, *Supplementary Text*).

Another potential limitation of our methods is that our motion exclusion threshold was liberal compared to other studies (44, 65). We extensively investigated this problem in another dataset (46), which guided the selection of this threshold. The key trade-off underlying this decision is between signal quality and data retention. A more liberal threshold means a higher retention rate, which makes this work more feasible in terms of time and cost, and less likely to introduce a selection bias, as mentioned above. Critically, although it may add noise, we do not expect this threshold to introduce a bias between conditions. Because our data are released publicly, this work can be reanalyzed to support the development of standards for motion exclusion in awake infants.

A final potential limitation is that our planned ROI analyses were not corrected for multiple comparisons. Even so, we found that the family of results was unlikely to be obtained by chance (see *SI Appendix*, *Supplementary Text*). Moreover, we found consistent evidence from multiple analyses implicating frontal regions like the MFG and ACC in attention, supporting our findings that attention recruits infant frontal cortex.

In sum, we found that frontal regions from adult frontoparietal and cingulo-opercular networks are recruited to support stimulus-driven attention in infants. This study adds to the growing evidence that the frontal cortex supports infant cognition, despite undergoing substantial and protracted anatomical development (35, 54). Functionality of frontal cortex is honed over the course of development to support complex operations (57), but these regions may be sufficiently developed in infancy to support stimulus-driven attention. This could reflect the importance of attention as a building block for learning and cognition, both in infancy and beyond.

Materials and Methods

Participants. Data from 24 sessions with infants aged 3.6 mo to 11.3 mo (M = 7.2; 14 female) met our minimum criterion for inclusion of four trials per condition. This sample does not include data from 11 sessions with participants in this age range that failed to produce enough data to reach criterion. Of the excluded sessions, three failed to meet the minimum number of trials, and the rest collected enough trials but fell below criterion after exclusions for head motion and gaze coding. In the final sample, four infants provided two sessions of usable data. This occurred because we tend to invite participating families to return if interested. Although we typically prioritize new experiments in these follow-up sessions, there are occasional opportunities to collect an additional session of the same task if these other experiments have been exhausted or were unsuccessful. Our philosophy is to make the most of scanning time with compliant infants, given how precious these subjects are. This also follows prior work that likewise treated multiple sessions from the same infant at different times as distinct data points (44, 46). We acknowledge that this decision could muddy statistical reasoning, but it reflects the unusually challenging nature of awake infant fMRI data collection and our belief that more data is better. These sessions typically occurred more than a month apart (range = 0.9 mo to 3.0 mo), so the data were treated separately, similar to prior work (44). Of the 24 sessions, five were collected at the Magnetic Resonance Research Center (MRRC), and the rest were collected at the Brain Imaging Center (BIC). Refer to *SI Appendix*, Table S1 for information on each session. Parents provided informed consent on behalf of their child. The study was approved by the Human Investigation Committee and the Human Subjects Committee at Yale University.

Materials. The code for running the cuing task can be found in GitHub at https://github.com/ntblab/experiment_menu. The code for the general analysis pipeline can be found here: https://github.com/ntblab/infant_neuropipe. The code for performing the specific analyses described in this paper can be found here: https://github.com/ntblab/infant_neuropipe/tree/PosnerCuing/. The data, including anonymized anatomical images, and both raw and preprocessed functional images can be found at https://doi.org/10.5061/dryad.sn02v6x36.

Data Acquisition. Data were acquired with a Siemens Prisma (3 T) MRI at both the MRRC and BIC sites with the 20-channel Siemens head coil. Anatomical images were acquired with a T1-weighted pointwise encoding time reduction with radial acquisition (PETRA) sequence (TR_1 = 3.32 ms, TR_2 = 2,250 ms, TE = 0.07 ms, flip angle = 6°, matrix = 320 × 320, slices = 320, resolution = 0.94 mm isotropic radial slices = 30,000). Functional images were acquired with a whole-brain T2* gradient-echo echo planar imaging (EPI) sequence (MRRC: TR = 2 s, TE = 28 ms, flip angle = 71°, matrix = 64 × 64, slices = 36, resolution = 3 mm isotropic, interleaved slice acquisition; BIC: identical except TE = 30 ms, slices = 34).

Procedures. Conducting fMRI research with awake infants is challenging for multiple reasons. Our protocol is described and validated in a separate methods paper (46). In brief, families visited the laboratory prior to their initial scanning session for an orientation session. This acclimated the infant and parent to the scanning environment. Scanning sessions were scheduled for a time when the parents felt the infant would be compliant. The infant and parent were extensively screened for metal. Hearing protection was applied to the infant in three layers: silicon inner ear putty, over-ear adhesive covers, and earmuffs. The infant was placed on the scanner bed, on top of a vacuum pillow that reduced movement comfortably. The top of the head coil was not used because the bottom elements provided sufficient coverage of the infant's head. This increased visibility for monitoring infant comfort and allowed us to project stimuli onto the ceiling of the bore directly above the infant's face using a custom mirror system. Using only the bottom of the head coil could have resulted in decreased data quality. However, detailed analyses revealed high-quality signal with this setup even in anterior regions of the infant brain farthest from the bottom head coil, likely as a result of their smaller head size (46). A video camera (MRRC: MRC

12 M-i camera; BIC: MRC high-resolution camera) recorded the infant's face during scanning for monitoring and offline gaze coding.

When the infant was calm and focused, stimuli were shown in MATLAB using Psychtoolbox (http://psychtoolbox.org/). The stimuli were pastel-colored shapes (4). Specifically, the attention getter was a multicolored square that oscillated in size from 2.5° to 7.5° at 1 Hz. The cue was a green triangle that was 3° wide by 1.5° high. The target was a multicolored pinwheel that rotated at 1 Hz and subtended 10°.

Each trial began with the attention getter. An experimenter in the control room monitored the participant's eyes, and, when the participant was looking at the screen, the experimenter pressed a key to trigger a trial that began at the start of the next TR pulse. This meant the fixation was of variable length. Once triggered, the fixation was removed and the cue was shown for 100 ms. The cue was presented 10° to the left, right, or both sides of fixation. After the cue offset, the screen was blank for 100 ms before the target appeared. The target was also centered 10° either to the left or right of fixation. The target was on screen for 2 s, after which the screen went blank until the next trial was initiated.

There were three trial types: valid, invalid, and neutral. On valid trials, the cue and target were presented on the same side. On invalid trials, cue and target were presented on opposite sides. On neutral trials, cues were presented bilaterally and the target appeared at one of those locations. Trials were divided into blocks, each containing eight trials randomly intermixed (four valid, two invalid, and two neutral), with cue and target side counterbalanced within each condition. Our goal was to collect four blocks per session, but we collected more if we thought that a block might be unusable (M = 4.7 blocks, range = 4 to 7). There was at least 6 s of rest between blocks, where the screen was blank.

Offline Gaze Coding. The gaze behavior of each infant was coded offline by two or three coders (M = 2.3) who were blind to the condition. The coders determined whether the gaze was oriented "left," "right," "center," "offscreen" (i.e., blinking or looking away), or "undetected" (i.e., out of the camera's field of view or obscured by a hand or other object). For frames in which only the attention getter was on the screen and nothing else, the coder was told that the infant was "probably looking at center." This helped to calibrate the coder but did not prevent them deviating from the instruction if they were confident the child was looking elsewhere. Coders were instructed to label frames according to where they thought the eyes were directed. This protocol meant that coders often changed the label midsaccade when the participant had looked left or right "enough." We used this protocol to be consistent across experiments where the instantaneous position of the eye, rather than the trajectory, was important. We could have alternatively instructed coders to only change the label when the saccade was completed. Our protocol, compared to this alternative, would have shorter estimates of RT. Critically, this possibility does not introduce a bias between trial conditions.

Every video frame of each infant was coded at least once across coders. The frame rate and resolution varied by camera and site, but the minimum rate was 16 Hz, and the resolution was always sufficient to identify the eye. The label for each frame was determined as the mode of a moving window of five frames centered on that frame across all coder reports. In case of a tie, the modal response from the previous frame was used. The coders were highly reliable: When coding the same frame, coders reported the same response on 84% (range across sessions = 64 to 99%) of frames. Trials were excluded if the participant was not looking for the majority of the time during the cue presentation, if they looked to the target location before its onset, or if they did not look at the target within 1,000 ms of its onset.

Preprocessing. Individual runs were preprocessed using FEAT in FSL (https://fsl.fmrib.ox.ac.uk/fsl), with a modified pipeline for infant data. Three volumes were discarded from the beginning of each run, in addition to the volumes automatically discarded by the EPI sequence. Blocks were stripped of any excess burn-in or burn-out volumes greater than the 3 TRs (6 s) of rest after each block. Pseudo-runs were created if other experiments, not discussed here, were started in a run with the data of interest (sessions with a pseudo-run, N = 20). Blocks were sometimes separated by long breaks (>30 s) within a session because the participant was taken out of the scanner, because an anatomical scan was collected, or because of intervening experiments (N = 8; M = 391.1 s break; range = 63.7 s to 1342.8 s). The reference volume for alignment and motion correction was the "centroid" volume that had the minimal Euclidean distance from all other volumes. The slices in each volume were realigned using slice time correction. Time points were excluded when there was greater than 3 mm of movement from the previous time point (M = 11.7%, range = 0.0 to 32.6%). This threshold can be considered liberal by comparison to past studies (44, 65). For an extended consideration of how motion thresholds affect signal quality and data retention, please refer to a recent methods paper we published (46). We interpolated rather than removed these time points so that they did not bias the linear detrending (in later analyses, these time points were ignored). Blocks were excluded if more than 50% of the time points were excluded. To determine which voxels were brain and which were nonbrain, we created a mask from the signal-to-fluctuating-noise ratio for each voxel in the centroid volume. The data were smoothed with a Gaussian kernel (5 mm full width at half maximum) and linearly filtered in time. AFNI's (https://afni.nimh.nih.gov) despiking algorithm was used to attenuate aberrant time points within voxels. For further explanation and justification of this preprocessing procedure, refer to ref. 46.

We aligned each run's centroid volume to the infant's anatomical scan from the same session. We used FLIRT with a normalized mutual information cost function to create the initial alignment with six degrees of freedom (DOF). Additional manual alignment was then performed using mrAlign from mrTools (Gardner Lab) to fix deficiencies of automatic alignment. In particular, we used landmarks like the border between the cerebellum and occipital cortex, the eyeballs/eye sockets, and ventricles to guide our alignment. The preprocessed functional data were aligned into anatomical space but retained their original spatial resolution (3 mm isotropic). The anatomical scan from each session was automatically aligned (FLIRT) to an age-appropriate MNI infant template using 12 DOF (66). In particular, we used three different atlases covering the age ranges 2 mo to 5 mo, 5 mo to 8 mo, and 8 mo to 11 mo, and used the appropriate atlas for each participant. This alignment was manually adjusted using nine DOF in Freeview and the same landmarks used for aligning functional data to anatomical space. The data were then aligned to the adult MNI template (MNI152) using a predefined transformation (12 DOF). This pipeline allowed the functional data to be transformed into standard space. ROI and whole-brain voxelwise analyses were performed in this 1 mm MNI space. To determine which voxels to consider at the group level, the intersection of brain voxels from all infant sessions in standard space was used as a mask.

Sessions were considered usable if they had at least four usable trials of each condition. In the final sample, and consistent with the frequency of trial types, participants had an average of 12.9 (range: 8 to 18) valid trials, 6.7 (range: 4 to 10) neutral trials, and 6.6 (range: 4 to 10) invalid trials. A similar inclusion rate was observed across trial types: 70% of valid trials, 73% of neutral trials, and 72% of invalid trials were retained.

To account for differences in intensity and variance across runs, the blocks that survived exclusions were normalized over time within run using z scoring, prior to the runs being concatenated for further analyses.

Behavior Analysis. We quantified the RT for the participant to saccade to the target. In particular, the onset time of the target was subtracted from the time stamp of the frame when the participant first looked to the correct side (i.e., left if the target was on the left). Only trials that met the inclusion criteria (e.g., low head motion, looking during the cue presentation) were retained for analysis. The RT for each trial was averaged within condition and then compared across sessions. Nonparametric bootstrap resampling was used to compare the conditions (67). Namely, for each test, we sampled 24 sessions with replacement 10,000 times, computing the mean across participants on each iteration to generate a sampling distribution. For null hypothesis testing, we calculated the P value as the proportion of samples where the mean was in the opposite direction from the true effect, doubled to make the test two-tailed. A similar bootstrap resampling procedure was used to statistically evaluate the correlation between age and behavior: The age and behavior bivariate data from each participant were sampled with replacement 10,000 times, and, for each sample, the Pearson correlation was calculated. The P value was the proportion of samples resulting in a correlation with the opposite sign from the true correlation, doubled to make the test two-tailed. We also performed a follow-up analysis using only the first block of usable data. One participant did not have any usable invalid trials in their first block, so they were not included in statistical comparisons involving invalid trials in this analysis.

GLM Analysis. For the main analysis, a GLM was fit to the preprocessed and z scored blood-oxygen-level-dependent activity using FEAT in FSL. Separate regressors were specified for valid, invalid, and neutral trials. An event of a given condition began at the onset of the cue and ended at the target offset. Each event was modeled as a boxcar (2.2 s duration), convolved with a double-gamma hemodynamic response function. The six translation and

rotation parameters from motion correction were included in the GLM as regressors of no interest. Excluded TRs were scrubbed with an additional regressor for each to-be-excluded time point (68). The main contrasts compared invalid greater than valid trials, neutral greater than valid trials, and invalid greater than neutral trials. The *z* statistic volumes corresponding to these three contrasts were extracted for each participant and aligned to standard space where subsequent analyses were performed. To visualize each contrast, we performed a voxelwise whole-brain *t* test across participants.

ROIs were defined with Neurosynth, a metaanalytic tool for identifying loci of activation from published fMRI studies (49). Specifically, we acquired the statistic map for the term "attention" on December 1, 2019. This aggregated across 1,831 studies and used a false discovery rate of 0.01 to detect regions that were reliably implicated in attention. Using FSL's cluster algorithm, we identified nine clusters with at least 27 voxels: in ascending size, rTPJ, lIPS, rLOC, lLOC, rACC, lFEF, lSPL, rFEF, and rSPL (*SI Appendix*, Table S2). Lowercase "r" and "l" indicate left and right hemispheres, respectively. Because this is a functional atlas, rather than an anatomical atlas, some of these regions do not map cleanly onto anatomy, but the names were chosen to be consistent with other regions described in the literature. For instance, the ACC ROI includes large portions of the paracingulate cortex and may be instead described as medial cingulate cortex, which is part of the dorsal salience network (59). The atlas was in 2 mm isotropic space, so we upsampled it to 1 mm space to be consistent with our other data. We manually divided two of the ROIs since they included anatomically and theoretically distinct regions. Namely, we split off part of rFEF to make rMFG and part of rSPL to make rIPS. We collapsed ROIs bilaterally when available, such as lFEF and rFEF. The mean *z* statistic value across voxels within each ROI was computed for each participant and contrast. The statistical significance of each ROI and correlations with age were evaluated using bootstrap resampling (as described above). For follow-up analyses, we edited these ROIs in two ways. First, we performed one step of modal dilation to increase the size of each region while preserving its overall shape. Second, we created spherical ROIs around the peak voxel within each ROI. These spheres had a radius of 10 mm, resulting in a constant voxel count across regions, although the shape did not reflect the original ROI.

Data Availability. Anonymized fMRI data and summary behavioral data have been deposited in Dryad (https://doi.org/10.5061/dryad.sn02v6x36) (69). The code for performing the specific analyses described in this paper can be found on GitHub (https://github.com/ntblab/infant_neuropipe/tree/PosnerCuing/).

ACKNOWLEDGMENTS We thank all of the families who participated; N. Wilson, N. Córdova, and V. Bejjanki for help with initial setup; K. Armstrong, C. Greenberg, J. Bu, L. Rait, J. Daniels, and the entire Yale Baby School team for recruitment, scheduling, and administration; H. Faulkner, Y. Braverman, A. Klein, J. Fel, and J. Wu for help with gaze coding; and R. Lee, L. Nystrom, N. DePinto, and R. Watts for technical support. We are grateful for internal funding from the Department of Psychology and Princeton Neuroscience Institute at Princeton University and from the Department of Psychology and Faculty of Arts and Sciences at Yale University. N.B.T.-B. was further supported by the Canadian Institute for Advanced Research.

1. E. J. Gibson, Exploratory behavior in the development of perceiving, acting, and the acquiring of knowledge. *Annu. Rev. Psychol.* **39**, 1–42 (1988).
2. R. Baillargeon, Object permanence in 31/2-and 41/2-month-old infants. *Dev. Psychol.* **23**, 655 (1987).
3. R. N. Aslin, P. Salapatek, Saccadic localization of visual targets by the very young human infant. *Atten. Percept. Psychophys.* **17**, 293–302 (1975).
4. M. H. Johnson, M. I. Posner, M. K. Rothbart, Facilitation of saccades toward a covertly attended location in early infancy. *Psychol. Sci.* **5**, 90–93 (1994).
5. T. Farroni, S. Massaccesi, D. Pividori, M. H. Johnson, Gaze following in newborns. *Infancy* **5**, 39–60 (2004).
6. L. L. Emberson, J. E. Richards, R. N. Aslin, Top-down modulation in the infant brain: Learning-induced expectations rapidly affect the sensory cortex at 6 months. *Proc. Natl. Acad. Sci. U.S.A.* **112**, 9585–9590 (2015).
7. M. Corbetta, G. L. Shulman, Control of goal-directed and stimulus-driven attention in the brain. *Nat. Rev. Neurosci.* **3**, 201–215 (2002).
8. F. Doricchi, E. Macci, M. Silvetti, E. Macaluso, Neural correlates of the spatial and expectancy components of endogenous and stimulus-driven orienting of attention in the Posner task. *Cerebr. Cortex* **20**, 1574–1585 (2010).
9. C. M. Arrington, T. H. Carr, A. R. Mayer, S. M. Rao, Neural mechanisms of visual attention: Object-based selection of a region in space. *J. Cognit. Neurosci.* **12**, 106–117 (2000).
10. M. Corbetta, G. Patel, G. L. Shulman, The reorienting system of the human brain: From environment to theory of mind. *Neuron* **58**, 306–324 (2008).
11. N. U. Dosenbach *et al.*, Distinct brain networks for adaptive and stable task control in humans. *Proc. Natl. Acad. Sci. U.S.A.* **104**, 11073–11078 (2007).
12. G. L. Shulman *et al.*, Interaction of stimulus-driven reorienting and expectation in ventral and dorsal frontoparietal and basal ganglia-cortical networks. *J. Neurosci.* **29**, 4392–4407 (2009).
13. B. Casey, N. Tottenham, C. Liston, S. Durston, Imaging the developing brain: What have we learned about cognitive development? *Trends Cognit. Sci.* **9**, 104–110 (2005).
14. N. Gogtay *et al.*, Dynamic mapping of human cortical development during childhood through early adulthood. *Proc. Natl. Acad. Sci. U.S.A.* **101**, 8174–8179 (2004).
15. J. Matsuzawa *et al.*, Age-related volumetric changes of brain gray and white matter in healthy infants and children. *Cerebr. Cortex* **11**, 335–342 (2001).
16. J. H. Gilmore *et al.*, Longitudinal development of cortical and subcortical gray matter from birth to 2 years. *Cerebr. Cortex* **22**, 2478–2485 (2012).
17. K. Farrant, L. Q. Uddin, Asymmetric development of dorsal and ventral attention networks in the human brain. *Dev. Cognit. Neurosci.* **12**, 165–174 (2015).
18. K. Konrad *et al.*, Development of attentional networks: An fMRI study with children and adults. *Neuroimage* **28**, 429–439 (2005).
19. S. Alcauter, W. Lin, J. K. Smith, J. H. Gilmore, W. Gao, Consistent anterior–posterior segregation of the insula during the first 2 years of life. *Cerebr. Cortex* **25**, 1176–1187 (2015).
20. M. Eyre *et al.*, The developing human connectome project: Typical and disrupted functional connectivity across the perinatal period. bioRxiv [Preprint] (2020). https://doi.org/10.1101/2020.01.20.912881 (Accessed 11 August 2020).
21. W. Gao et al., Evidence on the emergence of the brain's default network from 2-week-old to 2-year-old healthy pediatric subjects. *Proc. Natl. Acad. Sci. U.S.A.* **106**, 6790–6795 (2009).
22. W. Gao *et al.*, Functional network development during the first year: Relative sequence and socioeconomic correlations. *Cerebr. Cortex* **25**, 2919–2928 (2015).
23. N. Padilla *et al.*, Intrinsic functional connectivity in preterm infants with fetal growth restriction evaluated at 12 months corrected age. *Cerebr. Cortex* **27**, 4750–4758 (2017).
24. M. N. Spann, C. Monk, D. Scheinost, B. S. Peterson, Maternal immune activation during the third trimester is associated with neonatal functional connectivity of the salience network and fetal to toddler behavior. *J. Neurosci.* **38**, 2877–2886 (2018).
25. J. de Fockert, G. Rees, C. Frith, N. Lavie, Neural correlates of attentional capture in visual search. *J. Cognit. Neurosci.* **16**, 751–759 (2004).
26. J. M. Kincade, R. A. Abrams, S. V. Astafiev, G. L. Shulman, M. Corbetta, An event-related functional magnetic resonance imaging study of voluntary and stimulus-driven orienting of attention. *J. Neurosci.* **25**, 4593–4604 (2005).
27. K. N. Meyer, F. Du, E. Parks, J. B. Hopfinger, Exogenous vs. endogenous attention: Shifting the balance of fronto-parietal activity. *Neuropsychologia* **111**, 307–316 (2018).
28. K. V. Jakobsen, J. E. Frick, E. A. Simpson, Look here! The development of attentional orienting to symbolic cues. *J. Cognit. Dev.* **14**, 229–249 (2013).
29. B. M. Hood, J. D. Willen, J. Driver, Adult's eyes trigger shifts of visual attention in human infants. *Psychol. Sci.* **9**, 131–134 (1998).
30. G. Csibra, L. A. Tucker, M. H. Johnson, Neural correlates of saccade planning in infants: A high-density ERP study. *Int. J. Psychophysiol.* **29**, 201–215 (1998).
31. M. Scaife, J. S. Bruner, The capacity for joint visual attention in the infant. *Nature* **253**, 265–266 (1975).
32. M. I. Posner, M. K. Rothbart, B. E. Sheese, P. Voelker, Control networks and neuromodulators of early development. *Dev. Psychol.* **48**, 827 (2012).
33. A. Berger, G. Tzur, M. I. Posner, Infant brains detect arithmetic errors. *Proc. Natl. Acad. Sci. U.S.A.* **103**, 12649–12653 (2006).
34. G. Dehaene-Lambertz, E. S. Spelke, The infancy of the human brain. *Neuron* **88**, 93–109 (2015).
35. G. Raz, R. Saxe, Learning in infancy is active, endogenously motivated, and depends on the prefrontal cortices. *Annu. Rev. Dev. Psychol.* **2**, 247–268 (2020).
36. W. Xie, J. E. Richards, The relation between infant covert orienting, sustained attention and brain activity. *Brain Topogr.* **30**, 198–219 (2017).
37. W. Xie, B. M. Mallin, J. E. Richards, Development of infant sustained attention and its relation to EEG oscillations: An EEG and cortical source analysis study. *Dev. Sci.* **21**, e12562 (2018).
38. Á. Conejero, S. Guerra, A. Abundis-Gutiérrez, M. R. Rueda, Frontal theta activation associated with error detection in toddlers: Influence of familial socioeconomic status. *Dev. Sci.* **21**, e12494 (2018).
39. S. Lloyd-Fox *et al.*, Habituation and novelty detection fNIRS brain responses in 5-and 8-month-old infants: The Gambia and UK. *Dev. Sci.* **22**, e12817 (2019).
40. J. Colombo, The development of visual attention in infancy. *Annu. Rev. Psychol.* **52**, 337–367 (2001).
41. M. H. Johnson, M. I. Posner, M. K. Rothbart, Components of visual orienting in early infancy: Contingency learning, anticipatory looking, and disengaging. *J. Cognit. Neurosci.* **3**, 335–344 (1991).
42. A. B. Clohessy, M. I. Posner, M. K. Rothbart, S. P. Vecera, The development of inhibition of return in early infancy. *J. Cognit. Neurosci.* **3**, 345–350 (1991).
43. L. Biagi, S. A. Crespi, M. Tosetti, M. C. Morrone, BOLD response selective to flow-motion in very young infants. *PLoS Biol.* **13**, e1002260 (2015).
44. B. Deen *et al.*, Organization of high-level visual cortex in human infants. *Nat. Commun.* **8**, 13995 (2017).
45. G. Dehaene-Lambertz, S. Dehaene, L. Hertz-Pannier, Functional neuroimaging of speech perception in infants. *Science* **298**, 2013–2015 (2002).

46. C. T. Ellis *et al.*, Re-imagining fMRI for awake behaving infants. *Nat. Commun.* **11** (2020).
47. S. Ross-Sheehy, S. Schneegans, J. P. Spencer, The infant orienting with attention task: Assessing the neural basis of spatial attention in infancy. *Infancy* **20**, 467–506 (2015).
48. M. I. Posner, M. J. Nissen, W. C. Ogden, "Attended and unattended processing modes: The role of set for spatial location" in *Modes of Perceiving and Processing Language*, H. L. Pick, I. J. Saltzman, Eds. (Eribaum, Hillsdale, NJ, 1978), pp 131–157.
49. T. Yarkoni, R. A. Poldrack, T. E. Nichols, D. C. Van Essen, T. D. Wager, Large-scale automated synthesis of human functional neuroimaging data. *Nat. Methods* **8**, 665–670 (2011).
50. C. T. Ellis, N. B. Turk-Browne, Infant fMRI: A model system for cognitive neuroscience. *Trends Cognit. Sci.* **22**, 375–387 (2018).
51. M. Esterman, B. J. Tamber-Rosenau, Y. C. Chiu, S. Yantis, Avoiding non-independence in fMRI data analysis: Leave one subject out. *Neuroimage* **50**, 572–576 (2010).
52. R. Perry, S. Zeki, The neurology of saccades and covert shifts in spatial attention: An event-related fMRI study. *Brain* **123**, 2273–2288 (2000).
53. P. U. Tse, F. J. Baumgartner, M. W. Greenlee, Event-related functional MRI of cortical activity evoked by microsaccades, small visually-guided saccades, and eyeblinks in human visual cortex. *Neuroimage* **49**, 805–816 (2010).
54. C. T. Ellis *et al.*, Evidence of hippocampal learning in human infants. bioRxiv [Preprint] (2020). https://doi.org/10.1101/2020.10.07.329862 (Accessed 10 October 2020).
55. M. D. Fox, M. Corbetta, A. Z. Snyder, J. L. Vincent, M. E. Raichle, Spontaneous neuronal activity distinguishes human dorsal and ventral attention systems. *Proc. Natl. Acad. Sci. U.S.A.* **103**, 10046–10051 (2006).
56. E. K. Miller, J. D. Cohen, An integrative theory of prefrontal cortex function. *Annu. Rev. Neurosci.* **24**, 167–202 (2001).
57. Y. Munakata, H. R. Snyder, C. H. Chatham, Developing cognitive control: Three key transitions. *Curr. Dir. Psychol. Sci.* **21**, 71–77 (2012).
58. C. M. Thiel, K. Zilles, G. R. Fink, Cerebral correlates of alerting, orienting and reorienting of visuospatial attention: An event-related fMRI study. *Neuroimage* **21**, 318–328 (2004).
59. A. Touroutoglou, M. Hollenbeck, B. C. Dickerson, L. F. Barrett, Dissociable large-scale networks anchored in the right anterior insula subserve affective experience and attention. *Neuroimage* **60**, 1947–1958 (2012).
60. I. Indovina, E. Macaluso, Dissociation of stimulus relevance and saliency factors during shifts of visuospatial attention. *Cerebr. Cortex* **17**, 1701–1711 (2007).
61. E. Natale, C. A. Marzi, E. Macaluso, fMRI correlates of visuo-spatial reorienting investigated with an attention shifting double-cue paradigm. *Hum. Brain Mapp.* **30**, 2367–2381 (2009).
62. E. Natale, C. Marzi, E. Macaluso, Right temporal-parietal junction engagement during spatial reorienting does not depend on strategic attention control. *Neuropsychologia* **48**, 1160–1164 (2010).
63. D. M. Small *et al.*, Monetary incentives enhance processing in brain regions mediating top-down control of attention. *Cerebr. Cortex* **15**, 1855–1865 (2005).
64. J. Dubois, R. Adolphs, Building a science of individual differences from fMRI. *Trends Cognit. Sci.* **20**, 425–443 (2016).
65. J. D. Power *et al.*, Methods to detect, characterize, and remove motion artifact in resting state fMRI. *Neuroimage* **84**, 320–341 (2014).
66. V. S. Fonov, A. C. Evans, R. C. McKinstry, C. Almli, D. Collins, Unbiased nonlinear average age-appropriate brain templates from birth to adulthood. *Neuroimage* **47**, S102 (2009).
67. B. Efron, R. Tibshirani, Bootstrap methods for standard errors, confidence intervals, and other measures of statistical accuracy. *Stat. Sci.* **1**, 54–75 (1986).
68. J. S. Siegel *et al.*, Statistical improvements in functional magnetic resonance imaging analyses produced by censoring high-motion data points. *Hum. Brain Mapp.* **35**, 1981–1996 (2014).
69. C. T. Ellis, L. J. Skalaban, T. S. Yates, N. B. Turk-Browne, Attention recruits frontal cortex in human infants. Dryad. https://doi.org/10.5061/dryad.sn02v6x36. Deposited 2 March 2021.